Friction **7**(2): 129–142 (2019)
https://doi.org/10.1007/s40544-017-0194-2
ISSN 2223-7690
CN 10-1237/TH

RESEARCH ARTICLE

Tribology of WC reinforced SiC ceramics: Influence of counterbody

Sandan Kumar SHARMA[1], **B. Venkata MANOJ KUMAR**[1,*], **Young-Wook KIM**[2]

[1] *Department of Metallurgical and Materials Engineering, Indian Institute of Technology (IIT) Roorkee, Roorkee 247667, India*

[2] *TriboCeramics Laboratory, Department of Materials Science and Engineering, the University of Seoul, Seoul 130743, Republic of Korea*

Received: 23 June 2017 / Revised: 04 August 2017 / Accepted: 28 September 2017

Abstract: Hot pressed silicon carbide (SiC) composites prepared with 0, 10, 30 or 50 wt% tungsten carbide (WC) are subjected to dry sliding wear against WC-Co and steel ball. In particular an attempt has been made to answer the following important questions: (i) How does the load (from 5 to 20 N) effect sliding wear behaviour of SiC-ceramics against WC-Co and steel counterbodies? (ii) Is there any effect of WC content on friction and wear characteristics of SiC ceramics? (iii) Does the dominant material removal mechanism of SiC ceramics change with the addition of WC or counterbody? (iv) What is the influence of mechanical properties on the sliding wear? Experimental results indicated that coefficient of friction (COF) for the SiC ceramics varied between 0.66 and 0.33 with change in load and counterbodies. Wear volume for SiC ceramics found approximately 6–10 times more against WC-Co as compared against steel. Wear volume changes from 2.0×10^{-3} mm^3 to 1.2×10^{-2} mm^3 with change in counterbodies for SiC-(10, 30 or 50 wt%) WC composite at 20 N. SiC ceramics indicated abrasion and composites reveal tribochemical wear as major material removal mechanisms. Wear is influenced by the hardness of counterbody and fracture toughness of SiC-WC composites.

Keywords: silicon carbide; tungsten carbide; composites; steel; sliding wear; counterbody

1 Introduction

SiC based ceramics possess impressive properties like low density, high hardness, high temperature strength, and corrosion resistance and wear resistance even at higher temperature. They are attractive for various tribological applications such as bearings, mechanical seals, nozzles, turbine parts, heat exchangers, fusion reactor, cylinder liners, and cutting tools, etc. [1–5].

Many researchers have explored the potential of SiC ceramics and their composites in different tribological conditions [6]. It was found that the behaviour of SiC ceramics in sliding conditions is complex and dependent on material aspects as well as experimental parameters. Important material aspects that influence wear of ceramics are grain size, grain boundary toughness, residual stresses, hardness and fracture toughness [7–9], while influencing experimental parameters are applied load, sliding speed, environment and types of tribopairs [5, 6].

It is reported that liquid phase sintered (LPS) SiC with fine or elongated grains microstructure resulted in improved wear resistance [8–12]. Lopez et al. found that reduction in intergranular phase or weak second phase (additive phase) and fine grain size or high aspect ratio of grain improves wear resistance of LPS SiC [10]. These research results indicate a strong influence of composition (microstructure) and mechanical properties of the composites in different wear conditions. Zum-Gahr et al. estimated the tribological behaviour of SiC ceramics by oxidation reactions in the presence of oxygen and/or humidity

* Corresponding author: B. Venkata MANOJ KUMAR, E-mail: manojfmt@iitr.ac.in

in the surrounding atmosphere [13]. The possible oxidation reactions occur due to heat generated during friction in humid or lubricated sliding contact affect the tribological behaviour of SiC ceramics [13]. It was also pointed out that, as the humidity increased from 30% to 60%, the nature of damage changed from mechanical to tribochemical [14]. Formation of oxidative layer may act as a protective and destructive layer depending upon nature of sliding coupling material, applied load, sliding speed, etc. [15, 16]. Kumar et al. observed a change in wear mechanism as microcracking at 1 N to tribochemical wear at 13 N load for SiC ceramics having small amount of additives [17]. Hsu et al. [18] reported a change in wear mechanism from abrasion at a low speed of 1.9 mm/s and a low load of 2 N to intergranular fracture at high speed of 0.57 m/s and a high load of 360 N in air or water. Sliding couples of ceramic materials like silicon carbide, silicon nitride, alumina or zirconia exhibit high friction coefficients in unlubricated conditions [16]. Kovalcikova et al. [19] studied the influence of counterpart material like Si_3N_4, Al_2O_3, ZrO_2 and WC-Co on the friction and wear behaviour of SiC ceramics. They found mechanical wear and tribochemical reaction as major material removal mechanisms against any ceramic counterpart. Some previous studies on the wear behaviour of different SiC based ceramics against different counter body are summarized in Table 1.

In order to explore the potential of SiC-WC composites for their use in automotive and aerospace

Table 1 Summary of sliding wear results of SiC based ceramics against different counterbodies.

Test perform	Materials	Counterbody	Testing parameters	Friction and wear	Major findings	References
Sliding: Pin on disk	SiC pin	SiC disk	Unlubricated, Load: 50 N, Velocity: 0.2−4.0 m/s	COF: 0.5; Wear: 2.1×10^{-6} m^3/(N·m)	Tribo-oxidation and surface fracture were identified as the dominant deterioration mechanisms.	[20]
Sliding: Ball-on-disk	LPS-SiC disk	SiC ball	Unlubricated, Load: 1, 6, 13 N, Velocity: 0.21 m/s	COF: 0.56–0.22; Wear: 10^{-6}–10^{-5}m^3/(N·m)	COF decreased whereas wear rate increased with increased load. Surface grooving and microcracking occurred at low load. Tribochemical wear was dominant at 6 and 13 N loads for all the ceramics.	[17]
Sliding Ring on ring	SiC ring	SiC ring	Unlubricated, Load: 225, 450 N, Velocity: 0.5−5.5 m/s	COF: 0.2−0.5; Wear: (8.6−12.3) × 10^{-14} m^3/N·m	Wear surfaces exhibit plastic deformation, ploughing, and oxide film formation and removal.	[21]
Sliding: Pin on disk	SiC & SiC-C pin	SiC disk	Unlubricated; Load: 5 N; Velocity: 0.18 m/s; Sliding distance:108 m	COF: 0.28−0.5; Wear: (2.4−50) × 10^{-6} m^3/N·m	With addition of the graphite, friction of the SiC-C composite reduced, whereas the wear rate increased. Wear mechanisms dominated by fracture and three-body abrasion.	[22]
Sliding: Ball on disk	SiC-WC disk	SiC ball	Unlubricated; Load: 5, 10, 20 N; Velocity: 0.16 m/s; rpm: 500	COF: 0.4−0.5; Wear: (3.3−38) × 10^{-6} m^3/(N·m)	Mechanical fracture with micro-cracking found as major material removal mechanism. WC addition reduced fracture and grain pull-out for SiC-WC composites.	[12]
Reciprocating: Ball on disk	SiC disk	SiC or Al_2O_3 ball	Unlubricated; Load: 1−10 N; Frequency: 2.5−20 Hz; Stroke: 100−1,600 μm	COF: 0.1−0.63; Wear: (0.15−25) × 10^{-6} m^3/(N·m)	Friction reduced with increased humidity and was found lower against SiC compare to Al_2O_3. Wear rate is affected significantly by humidity and decreases by one order of magnitude for Al_2O_3/SiC system and by two orders of magnitude for SiC/SiC system. Wear started by grain pullout and microcracking initially and lead to tribo-oxidation as the main wear mechanism in steady state.	[23]

(Continued)

Test perform	Materials	Counterbody	Testing parameters	Friction and wear	Major findings	References
Reciprocating: Ball on disk	SiC-TiC & SiC-TiC-TiB_2 disk	Al_2O_3 ball	Unlubricated; Load: 10 N; Frequency: 10 Hz; Stroke: 0.2 mm and 0.8 mm	COF: 0.55−0.39; Linear Wear: 50−8 µm	Friction and Wear both reduced for SiC composites compare to SiC ceramics. One order of change is observed in wear rate. The formation of tribo-reaction layers reduces the wear rate and fluctuation in friction reduced significantly.	[24]
Sliding: Ball on disk	LPS-SiC disk	WC ball	Unlubricated; Load: 5, 10, 20 N; Velocity: 0.1 m/s; rpm: 500	COF: 0.4−0.5; Wear: (1.8−6.7) × 10^{-6} m^3/(N·m)	Microcracks induced fracture and pull-out are responsible for material removal. Easy deformation and removal of large amount of weak Y_2O_3 rich phase is attributed for high wear for the high additive ceramics.	[25]
Sliding: Ball on disk	LPS-SiC disk	Si_3N_4 ball	Paraffin oil; Load: 70 N; Velocity: 0.04 m/s; rpm: 100; 500 min	Linear Wear: 300 µm	Interlocking networks of elongated SiC grains provided improved wear resistance. Absence of a continuous secondary phase matrix, prevents massive grain pullout and hence material removal.	[26]
Reciprocating: Ball on disk	SiC disk	Si_3N_4 ball	Unlubricated and Water; Load: 2 N; Frequency: 5 Hz; Stroke: 5 mm and 0.8 mm; 1,800 s	COF: 0.24−0.12; Wear: (7.5−11.0) × 10^{-14} m^3/(N·m)	Friction and wear reduced under water lubrication. SiC is good material candidates for tribological components in water environment. Severe wear arise by mechanical cracking of grains under high friction-induced tensile stress.	[27]
Sliding: Ball on disk	SiC disk	Si_3N_4, Al_2O_3, ZrO_2 or WC-Co	Unlubricated; Load: 5 N; Velocity: 0.1 m/s; sliding distance 500 m	COF: 0.45−0.67; Wear: (1.6−45.2) × 10^{-6} m^3/(N·m)	Friction and wear rate observed minimum against ZrO_2 and maximum against Si_3N_4. The main wear mechanism found as mechanical wear (micro-fracture) and tribochemical reaction against all the counterpart materials.	[19]
Sliding: Ball on disk	SiC disk	SiC, WC-Co or Steel ball	Unlubricated; Load: 5, 10, 20 N; Velocity: 0.16 m/s; rpm: 500	COF: 0.33−0.66; Wear volume: 5.9×10^{-4} mm^3 and 1.7×10^{-2} mm^3	Small size debris get connected and formed tribochemical layer and led to reduction in friction and wear against WC-Co. Against steel, hard $FeWO_4$ debris at the contact resulted in higher friction for SiC-WC composites against steel ball. Wear is influenced by the hardness of the counterbody and fracture toughness of SiC-WC composites.	Present Study

industries as tribological structural component like seals, bearings or heat exchanger tubes, it is important to estimate the tribological performance of the composites. The tribological behaviour of the ceramics composites is systematically investigated in dry sliding conditions against cermets (WC-Co) and metal (steel) counterbody in the present work. In particular, the influence of WC content (0 to 50 wt%) and counterpart material on wear mechanisms is elucidated.

2 Experimental details

Powder mixtures containing SiC, (0 to 50 wt%) WC and 5 wt% (Al_2O_3-Y_2O_3-CaO) additives were hot

pressed at 1,800 °C and 40 MPa for 1 h in an argon atmosphere to obtain sintered samples of 30 mm in diameter and 4 mm in thickness. SiC ceramics with 0, 10, 30 or 50 wt% WC content are respectively designated as SW0, SW10, SW30 or SW50. Vickers hardness measured at 1.96 N load for the composites varied from 24.0 GPa to 26.3 GPa, whereas indentation fracture toughness estimated using Anstis formula [28] varied from 5.8 MPa·m$^{1/2}$ to 6.7 MPa·m$^{1/2}$. Maximum hardness obtained for SiC-30 wt% WC, while the fracture toughness was maximum for SiC-50 wt% WC. More details on composites compositions, method of preparation and microstructure/mechanical properties can be found in our previous report [11]. The sintered sample surfaces were polished to obtain an arithmetic average surface roughness (Ra) of 30–70 nm. Surface roughness characteristics of polished surfaces were studied using atomic force microscopy (AFM) analysis (NT-MDT NTEGRA, Moscow, Russia). Typical microstructures of etched and fractured SiC specimens prepared with 0 and 50 wt% WC particles are shown in Fig. 1. Etched microstructures exhibited a reduction in the average size of the near equi-axed SiC grains from 835 to 578 μm with 50 wt% WC addition.

The friction and wear behaviour of monolithic SiC and SiC-WC composite disks were studied against commercially available AFBMA Grade-10 WC-Co (diameter = 10 mm, hardness = 14 GPa) and AISI 52100 grade steel (diameter = 6.35 mm, hardness = 7 GPa) balls using a ball-on-disk tribometer (TR-201E-M2, DUCOM, Bangalore, India). Before tribological testing, the disk samples and balls were cleaned using acetone in an ultrasonic bath for 15 min, followed by drying in a hot air stream. The ball was kept stationary under the applied load to make a track radius of 6 mm, while the disk was rotated at 500 rpm (a linear speed of 0.16 m/s) for 30 min (total sliding distance of 283 m). Sliding wear tests were done in ambient conditions (27 ± 5 °C and 40% ± 5% RH) at three loads: 5, 10 and 20 N. The width and depth of the wear scars were measured using a stylus profilometer (SJ 400, Mitutoyo, Japan). At least 10 orthogonal measurements per track for each composition were made to obtain average values of width and depth of wear scars. Results of average width and depth were used for quantification of the extent of volumetric wear damage on the disk (V) using the following formula:

$$V = 2\pi \times r \times d \times w \tag{1}$$

where r is the radius of the circular wear scar, and w and d are the width and depth of the wear scar, respectively.

Averages of the estimated wear volume and coefficient of friction (COF) data are reported after conducting at least three sliding experiments. The worn surfaces were studied to identify the dominant wear type of material removal using scanning electron microscope (SEM) equipped with energy dispersive X-ray spectroscopy (EDS) (ULTRA plus, Carl Zeiss, Germany). Debris collected after wear test were analyzed using SEM and Raman spectroscopy to understand the effect of counterbody material on friction and wear behaviour of SiC-WC composites.

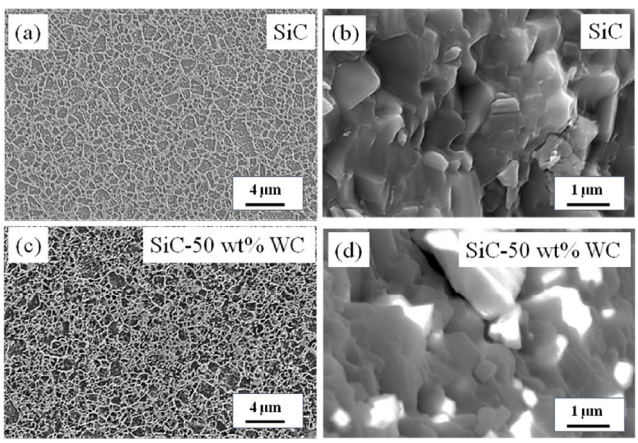

Fig. 1 SEM images of etched and fractured surface of SiC ceramics ((a) and (b)), and SiC ceramics reinforced with 50 wt% of WC ((c) and (d)).

3 Results

3.1 Friction results

Monolithic SiC ceramics subjected to sliding wear against different counterbody, i.e., WC-Co and Steel ball at 5 N, 10 N or 20 N, exhibited difference in frictional behavior (Fig. 2). It shows significant fluctuations in friction against WC-Co ball as compared to steel ball. Fluctuations reduced in their intensity with increase in load from 5 N to 20 N for any counterbody. Furthermore, monolithic SiC exhibited highest steady state COF value against WC-Co

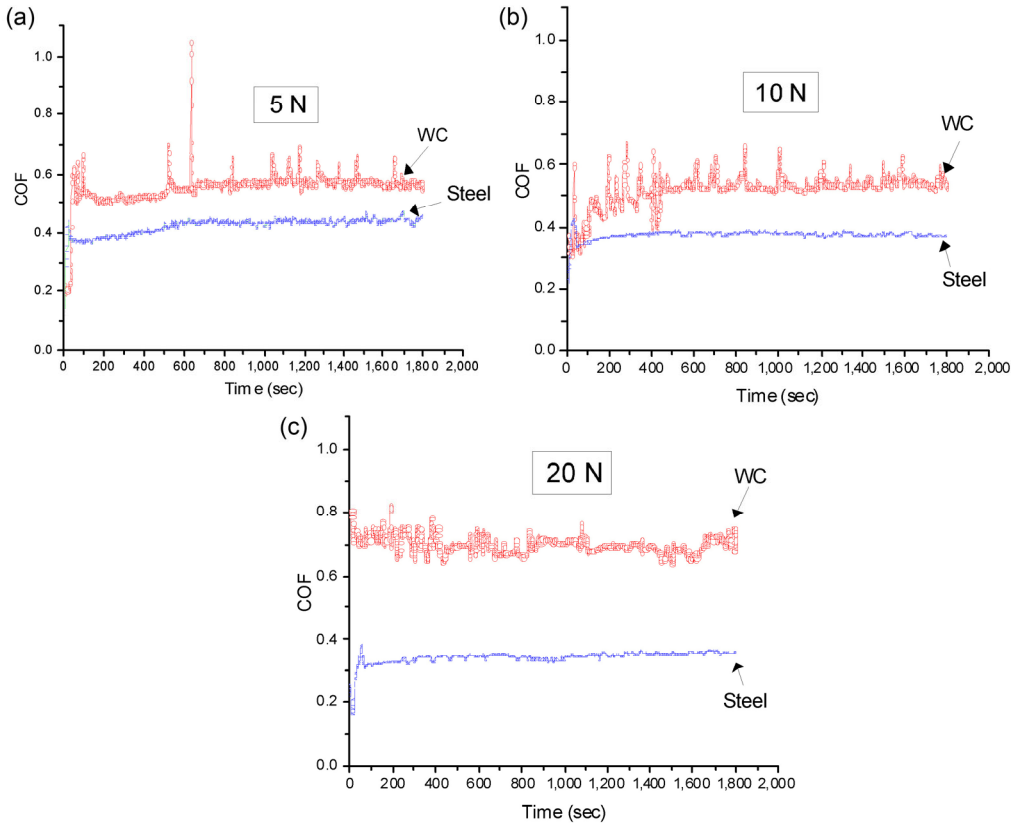

Fig. 2 Evolution of coefficient of friction for monolithic SiC ceramics at (a) 5 N; (b) 10 N and (c) 20 N, against WC-Co and steel counterbodies.

counterbody at any load. The difference between steady state value of COF against WC-Co and steel ball increased from ~0.15 to 0.36 as load increased from 5 N to 20 N.

Figure 3 shows the effect of WC content on the average steady state COF of SiC-WC composites when slid against WC-Co ball and steel ball at 20 N load. With increase in WC content average steady state COF decreased from 0.66 to 0.33 against WC-Co counterbody, whereas it increased from 0.34 to 0.43 against steel ball. Generally average COF value for SiC ceramics in sliding wear are reported from 0.20 to 0.75 with different parameters and working environments [6]. For ceramics, high friction results mechanical wear including third body abrasion, fracture and chipping [12, 13, 21], while less friction is observed with the formation of hydrated silica or adhered oxide layer at the contact [14, 20, 29]. Further, surface profiles of wear scar perpendicular to sliding direction are acquired for measuring depth and width of wear scar. Typical surface profiles of wear scars for monolithic

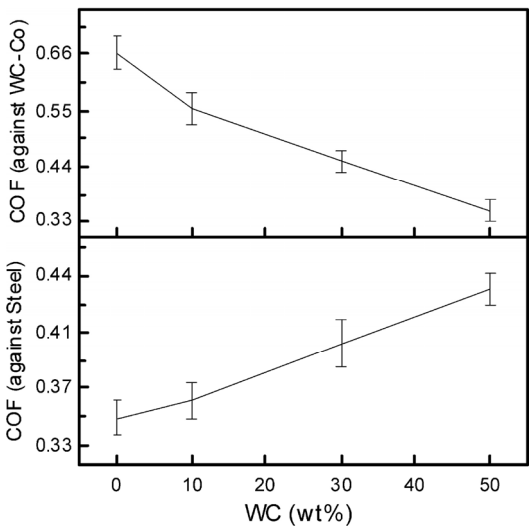

Fig. 3 Average coefficient of friction of SiC-WC composites against WC-Co and steel counterbodies at 20 N load.

SiC at 5, 10 or 20 N load and SiC-WC composites at 20 N load are respectively shown in Figs. 4 and 5. With an increase in load from 5 N to 20 N, depth and width varied from 0.23 μm to 1.53 μm and from

0.18 mm to 0.60 mm, respectively. At a given load, the depth and width of the scar are significantly higher against hard WC-Co counterbody as compared against steel counterbody (see Fig. 4).

It is observed from Fig. 5 that with increased WC content in SiC-WC composites, depth and width reduced against any ball at 20 N load. With increase in the WC content from 0 to 50 wt%, depth and width decrease from 0.69 μm to 0.28 μm and from 0.42 mm to 0.29 mm respectively against steel ball. Depth and width decreased from 1.53 μm to 1.18 μm and from 0.60 mm to 0.40 mm with increase in WC content against WC-Co ball. It is clear from the Figs. 4 and 5 that maximum value of width or depth obtained against WC-Co ball. Therefore, the depth and width of wear scars obtained during sliding wear of the SiC ceramics are dependent on hardness of the counterbody.

3.2 Wear results

The wear volume of SiC ceramics against WC-Co and steel ball at 5 N, 10 N and 20 N load is plotted in Fig. 6. In general, wear volume increased with increase in applied load against any counter body. SiC ceramics

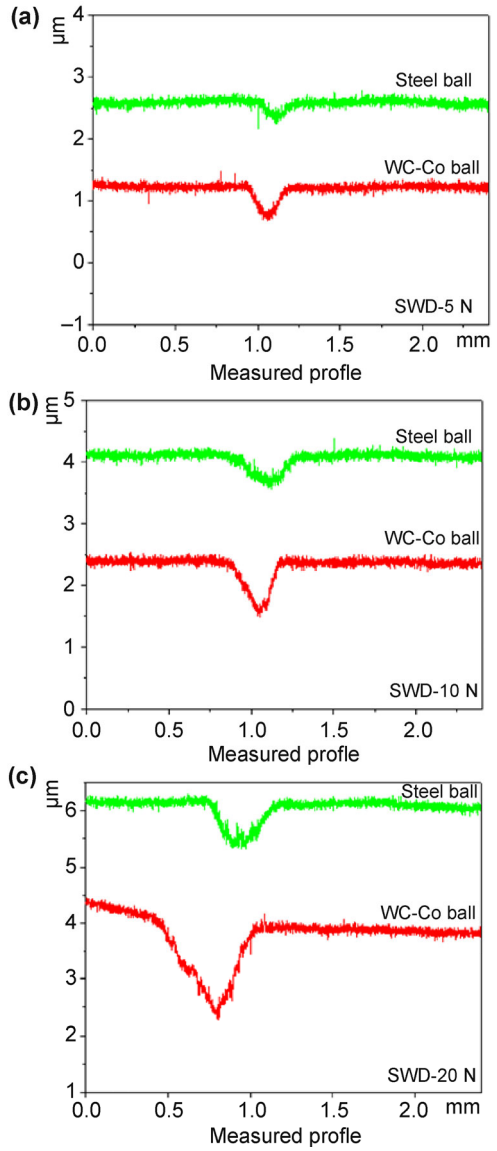

Fig. 4 Typical surface profile of wear scar on monolithic SiC ceramics at (a) 5 N, (b) 10 N and (c) 20 N, against WC-Co and steel counterbodies.

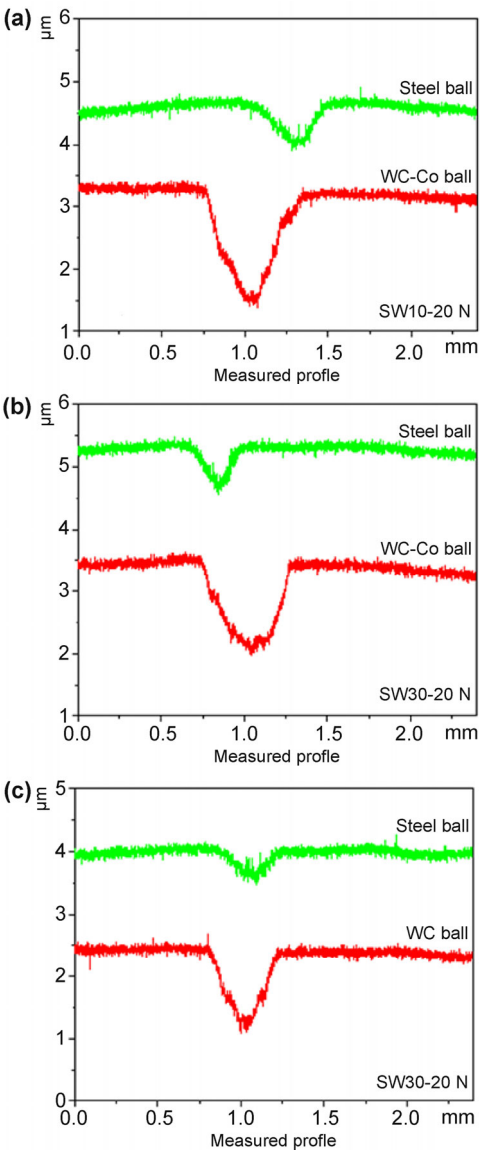

Fig. 5 Typical surface profile of wear scar against WC-Co and steel counterbodies at 20 N for different SiC ceramics sintered with (a) 10, (b) 30 and (c) 50 wt% WC.

exhibited approximately 5–10 times more wear against WC-Co counterbody as compared to against steel counterbody. The wear volume of SiC ceramics varied between 5.9 × 10^{-4} mm^3 and 1.7 × 10^{-2} mm^3 with change of load or counterbody. Against WC-Co ball, one order of magnitude increase in wear volume from 5.4 × 10^{-3} mm^3 to 1.7 × 10^{-2} mm^3 is observed with increased load. Similarly against steel ball, one order of magnitude increase in wear volume from 5.9 × 10^{-4} mm^3 to 4.7 × 10^{-3} mm^3 is obtained with increased load from 5 N to 20 N. It is also observed that SiC ceramics resulted in maximum wear at 20 N load against any counterbody. Therefore, SiC-WC composites are investigated only at 20 N load to understand the effect of reinforcement of WC particle on sliding wear behaviour against different counterbodies (WC-Co and steel ball).

Figure 7 shows the wear volume of SiC-WC composites as a function of WC content against WC-Co and steel counterbodies at 20 N. Lowest wear volume is obtained for SiC ceramics reinforced with 50 wt% WC against steel ball. It is to believe that SiC ceramics reinforced with large amount of WC exhibit higher fracture toughness that led to reduced mechanical fracture or grain pull-out during sliding wear. With increase in WC content from 10 to 50 wt%, wear volume decreased with one order of magnitude from 1.2 × 10^{-2} mm^3 to 5.7 × 10^{-3} mm^3 against WC-Co ball, whilea slight change in wear volume from 4.7 × 10^{-3} mm^3 to 2.0 × 10^{-3} mm^3 is observed against steel ball. Further, wear volume of counterbodies worn against SiC-WC composites at 20 N loadis shown in Fig. 8. It shows 4 to 5 times higher wear volume of steel ball as compared of WC-Co ball.

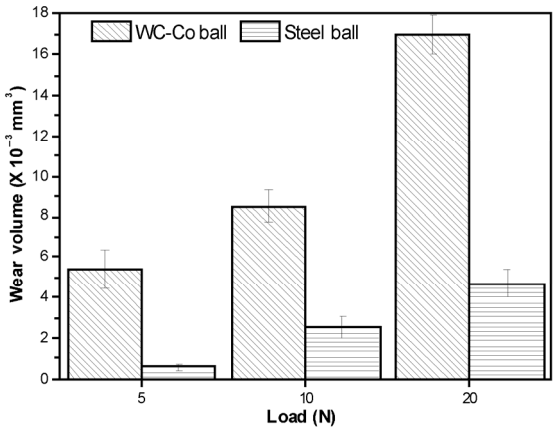

Fig. 6 Wear volume of SiC ceramics as function of load against WC-Co and steel counterbodies.

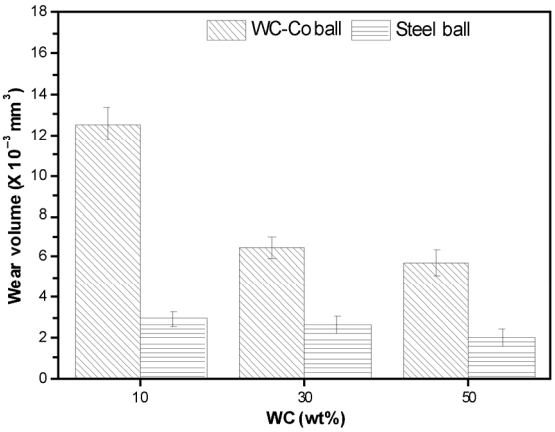

Fig. 7 Wear volume of SiC-WC composites against WC-Co and steel counterbodies at 20 N load as function of WC content.

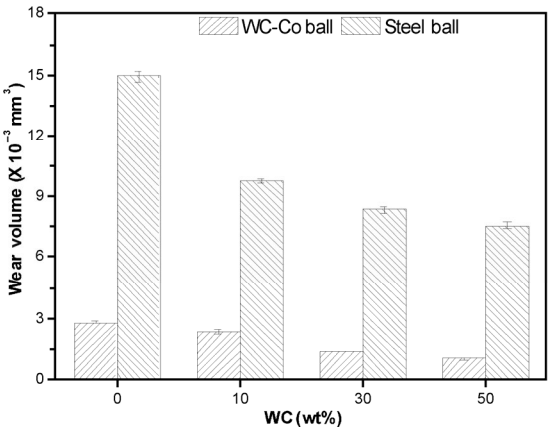

Fig. 8 Wear volumes of WC-Co and steel balls as a function of WC content at 20 N load.

3.3 Worn surface analysis

SEM images of SiC ceramics worn at 5, 10 and 20 N against WC-Co and steel ball are shown in Fig. 9. It is observed that extent of abrasion and retained debrison the disk surfaces increased with load against WC-Co ball. In case of steel counterbody, mild abrasion and retained debris are dominant on worn disk surface of SiC ceramics at low load of 5 N load while surface polishing and suppression of retained debris are observed at high load of 20 N. The EDS analysis of worn surfaces revealed the presence of oxygen along with elements of disk or counterbody (Figs. 9(g), 9(h), and 9(i)).

Figure 10 shows typical SiC-WC composites surfaces worn against WC-Co and steel counterbodies at 20 N load as a function of WC content. In case of WC-Co

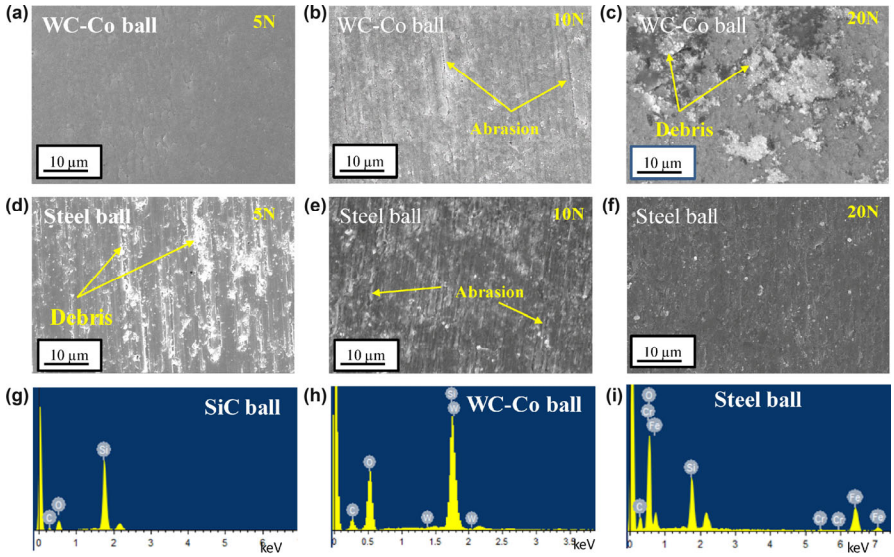

Fig. 9 SEM images of worn surfaces of SiC ceramics against WC-Co and steel counterbodies at 5 N, 10 N and 20 N load. EDS analysis of worn surface at 20 N against WC-Co and steel ball (g–i).

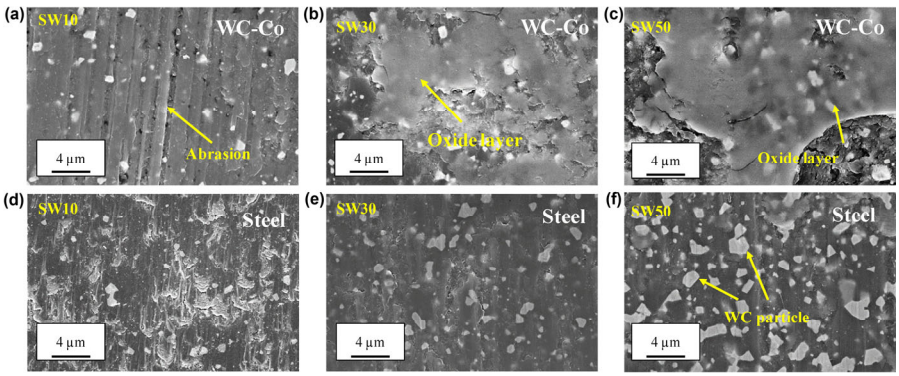

Fig. 10 SEM images of worn surfaces of SiC-WC composites against WC-Co and steel counterbodies at 20 N load.

counterbody, significant abrasion and WC particles or retained debris are observed on the worn surface of SiC-10 wt % WC composite, while the worn surface is covered with a thick layer in SiC-30 wt% WC and SiC-50 wt% WC composites (Figs. 10(a) to 10(c)). In case of steel counterbody, the SiC-10 wt % WC composite is rough with fracture surface and mild abrasion, while the reduced fracture and mild abrasion are observed on SiC-50 wt% WC composite worn surface (Figs. 10(c) to 10(f)). The presence of layer is not observed on the composite surface worn against steel.

Material removal mechanisms are further understood by observing surfaces of counterbody balls (Fig. 11) worn against SiC-WC composites at 20 N. It shows mainly polishing and adhered layer as material removal for any counterbody. Strongly adhered layer was observed on the WC-Co ball surfaces with the increased content of WC in SiC-WC composites. Against monolithic SiC ceramics, it is completely polished surface on steel ball (Fig. 11(e)) but, loosely adhered layers are also observed on ball surfaces with increased WC content in SiC-WC composites (Figs. 11(g) and 11(h)).

3.4 Debris analysis

SEM images of debris collected after wear of SiC-WC composites against WC-Co and steel balls are shown in Fig. 12. In general, debris size reduced with increase in WC content. This can be attributed to the reduced grain size of the SiC-WC composites with increase in WC content. Figure 13 shows Raman analysis of debris particles collected after sliding of

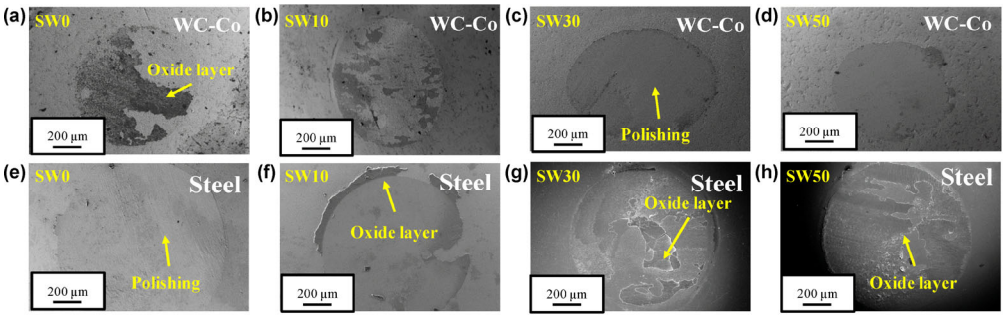

Fig. 11 SEM images of worn surfaces of counterbody (WC and steel ball) slid against SiC-WC composites at 20 N load.

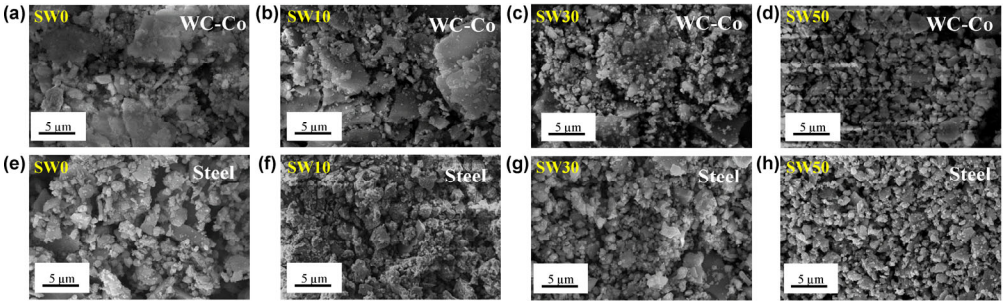

Fig. 12 SEM images of debris collected after wear of SiC-WC composites against WC-Co and steel counterbodies at 20 N load.

SW50 composite against WC-Co or steel counterbody. It validated the formation of silicon oxide [30], tungsten oxide [31] and cobalt tungsten oxide [32] when SiC-WC composites slid against WC-Co counterbody. In addition, it also supported the formation of iron oxide [33] and iron tungsten oxide [34] when SiC-WC composites slid against steel ball.

4 Discussion

In this section, phenomenological understanding on the effect of counterbody on frictional and wear behaviour of SiC-WC composites as function of WC content is provided. This is followed by the discussion on dominant mechanisms of material removal as function of counterbody and WC content. Also, a short note on the effect of mechanical properties on the wear behaviour of SiC-WC composites against different counterbody is provided.

4.1 Effect of counterbody on frictional and wear behaviour

Fluctuations in friction for monolithic SiC ceramics when slid against WC-Co ball are believed to be due to increased mechanical fracture or third body abrasion. Against steel ball, fluctuation reduced with increased load as iron oxide debris particles are

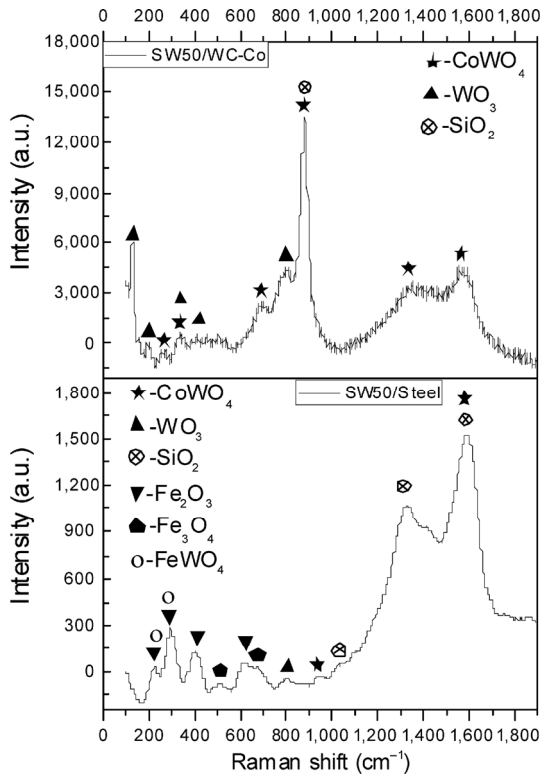

Fig. 13 Raman spectroscopy of debris collected after sliding wear of SW50 composites against WC-Co and steel counterbodies.

suppressed at higher load (see Figs. 2 and 8(f)). SiC ceramics exhibited highest average COF against WC-Co ball and lowest against steel ball at any load. It was reported earlier that ceramics with dissimilar sliding pairs exhibited different frictional behaviour due to difference in the ionic potential of oxides formed between mating surfaces in dry sliding conditions. The tendency for oxide layer formation is larger at high sliding loads due to friction induced high temperatures at the contact [29, 35].

In case of composites, reduced fracture with high WC content led to reduced tendency for the formation of hard oxides, hence less friction [19]. It is also well reported that [36–38] plastic deformation and transgranular fracture of individual grains were more pronounced in microstructures containing fine grains and resulted in small size debris. The small size debris particles were compressed and plastically deformed into layers during sliding contact and hence led to less friction and wear. For SiC-WC composites, fine grains are attributed to fine debris size. Fine debris particles are more prone to get connected to each other in hydrated environment and formed layers adherent with varying strengths to the material surface [13]. Strongly adhered layers resulted in less friction and protected the underneath material from wear. So fine grain SiC-WC composites exhibited lowest friction against WC-Co ball as compared to coarse grained monolithic SiC ceramics.

Increased friction obtained for SiC-WC/steel system contradicts to the reduction in friction with finer grains. During sliding against steel counterbody, formation of hard iron tungsten oxide ($FeWO_4$) is expected with increased WC content as follows:

$$2Fe + O_2 \rightarrow 2FeO \quad (2)$$

$$FeO + WO_3 \rightarrow FeWO_4 \quad (3)$$

Formation of hard $FeWO_4$ and loosely bonded iron oxide with WC content, participated as a third body between the mating surfaces and resulted in high friction during sliding of the composites against steel ball (see Figs. 3 and 13). So, it is worth to note that COF is dependent on nature of counterpart materials irrespective of their hardness.

Wear rates for SiC ceramics in sliding conditions varied in the order of 10^{-7}–10^{-4} mm^3/(N·m) [6]. Coarse grain SiC ceramics resulted to highest wear against any counterbody at 20 N load. Wear of disk surface reduced for fine grain SiC-WC composites with the formation of protective tribolayer on the disk/ball surface during sliding (see Figs. 10 and 11). The stability of adhered layers also reduced with increased average grain sizes of the ceramics and directed to cracking and/or delamination of the layers and hence increased the wear [36]. In the same set of sliding wear conditions, SiC-WC composites exhibited higher wear volume when slid against SiC counterbody compared to wear volume obtained in the present work [12]. Therefore, wear volume of SiC-WC composites is dependent on hardness of the counterbody ball. Steel balls with less hardness showed more wear than the harder WC-Co balls when slid against SiC-WC composites.

4.2 Wear mechanisms

Various types of mechanisms or types of material removal are reported in different wear conditions [39]. In the present study, with decreased hardness of counterbody, material removal mechanisms changed from mechanical fracture to tribochemical wear for the investigated ceramic composites. Extent of mechanical fracture for SiC ceramics is higher against WC-Co counterbody as compared to steel ball. Against steel counterbody, polishing of surface observed at higher load. The debris generated between the mating surfaces led to more wear due to third body abrasion for SiC ceramics at higher load. Major wear mode for SiC ceramics against WC-Co and steel counterbody at 5 N, 10 N and 20 N load are listed in Table 2.

The material removal from the disk surfaces caused due to deep penetration of counterbody in disk surfaces. As fracture toughness increases, abrasion (penetration) to the disk surfaces decreased with the

Table 2 Wear types for the SiC ceramics as function of load and counterbody.

Applied Load	Counterbody	
	Steel	WC-Co
5	Embedded debris and mild abrasion	Mild abrasion
10	Deep grooves mild abrasion	Deep grooves mild abrasion
20	Mild abrasion and polishing	Embedded debris and severe abrasion

increase in WC content, which led to decreased wear of SiC-WC composites against any counterbody. Strongly adhered tribolayer affected the frictional and wear characteristics of SiC-WC composites against WC-Co and steel ball. Adhered tribolayer protected the wear surface by restricting the depth of penetration during sliding. Lower penetration against counterbody having low hardness led to less removal of material. It implies that with decreased counterbody hardness from 28 GPa (for SiC ball) to 7 GPa (steel ball), wear of the SiC-WC composite reduced, as extent of abrasion, mechanical fracture and grain pull-out decreased with protective tribo layer (see Figs. 10(b), 10(c) and 11(g), 11(h)). Major mode of wear for the SiC-WC composites against WC-Co and steel ball with respect to WC content in SiC ceramics are summarized in Table 3. A schematic illustration of major material removal mechanisms for SiC ceramics and SiC-WC composites against WC-Co and steel counterbody are represented in Fig. 14.

Table 3 Wear types for the SiC-WC composites against WC-Co and steel ball as function of WC content.

WC content (wt%)	Counterbody	
	Steel	WC-Co
0	Mild abrasion and polishing	Embedded debris and severe abrasion
10	Mild abrasion and adhered debris	severe abrasion
30	Mild abrasion	Adhered and compacted oxide layer
50	Mild abrasion	Highly adhered and compacted layer

4.3 Effect of mechanical properties

The complex wear behaviour of brittle solids is often reported to be influenced by mechanical properties such as hardness, fracture toughness, and elastic modulus. Tatarko et al. [40] reported lower specific wear rate for the material with higher hardness. Moreover, Miyazaki [41] observed that neither hardness nor fracture toughness shows any direct relationship to the specific wear rate of Si_3N_4 ceramics. In the present study, the wear rate of studied materials decreased with the increased fracture toughness. The maximum hardness of 26.3 GPa for SiC-30 wt% WC composites is attributed to the homogeneous dispersion of WC particles in the SiC matrix. On the other hand, a maximum fracture toughness of 6.7 MPa·m$^{1/2}$ observed for SiC-50 wt% WC composites is attributed to crack deflection and bridging by a large amount of WC particles [11]. Results from the present study indicate that the minimum amount of material is removed for SiC-50 wt% WC composites against any counterbody, which possessed the maximum fracture toughness. Thus, fracture toughness appeared as more important property than hardness in estimating the extent of sliding wear for the investigated SiC-WC composites.

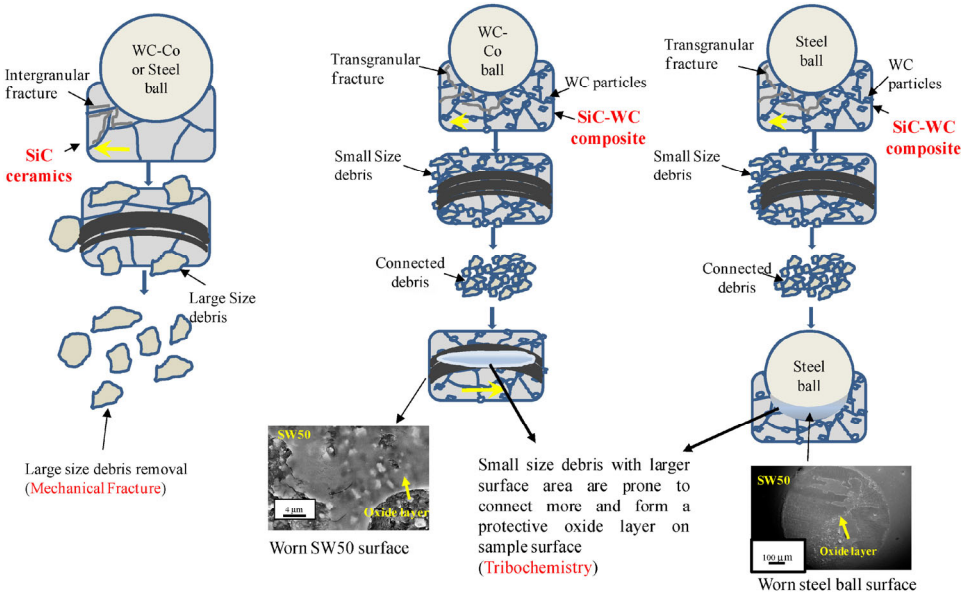

Fig. 14 Schematic illustration of wear mechanism for SiC ceramics and SiC-WC ceramics when slid against WC-Co or steel ball.

5 Conclusions

SiC ceramics were investigated for sliding wear behaviour against commercially available WC-Co or steel counterbody at 5 N, 10 N or 20 N load in ambient conditions using a ball-on-disk tribometer. Further, the effect of the addition of WC (10, 30 or 50 wt%) on the friction and wear characteristics of SiC-WC composites is studied against WC-Co or steel at 20 N load. The following are major conclusions:

(a) At high load, SiC ceramics resulted in higher friction against WC-Co ball due to increased fracture, while less friction observed at high load against steel ball due to the compaction of soft iron oxide debris. The COF value for the SiC ceramics varied between 0.66 against WC-Co ball and 0.34 against steel at 20 N load. SiC ceramics exhibited approximately 5–10 times more wear against WC-Co counterbody as compared against steel counterbody. Wear volume varied between 5.9×10^{-4} mm^3 and 1.7×10^{-2} mm^3 with change in load or counterbody. SEM-EDS analysis of worn surfaces of SiC ceramics indicated abrasive grooves with mechanical fracture responsible for the material removal against WC-Co ball, while abrasive grooves with polishing is observed against steel ball.

(b) With the increase in WC content from 10 to 50 wt %, average steady state COF decreased from 0.55 to 0.33 against WC-Co counterbody, while increased formation of hard $FeWO_4$ with increased amount of WC led to an increase in COF from 0.35 to 0.43 against steel. The SiC-WC composites with higher WC content exhibited less wear against any counterbody. Lowest wear volume of 2.0×10^{-3} mm^3 is obtained for SiC-50 wt% WC composites against steel ball.

(c) Worn surfaces of SiC-WC composites revealed tribochemistry with increased WC content. Fine grained SiC-WC composites exhibited small size debris. The compaction of which resulted in the formation of oxide rich layer at the contact. Raman spectroscopy analysis of debris collected from the worn surfaces of SiC-50 wt% WC composites indicated formation of silicon oxide, tungsten oxide, cobalt tungsten oxide particles when slid against WC-Co counterbody and additional formation of iron oxide and iron tungsten oxide against steel ball.

(d) The wear of SiC-WC composites is in general less against steel ball, whereas SiC-50 wt% WC composite with maximum fracture toughness of 6.7 MPa·m$^{1/2}$ exhibited superior wear resistance against any counterbody. The present study necessarily demonstrates that the wear is influenced by the hardness of the counterbody and fracture toughness of SiC-WC composites.

Acknowledgements

B.V. Manoj Kumar acknowledges partial support from Council of Scientific and Industrial Research (CSIR), New Delhi, India through project No. 22(0654)/14/EMR-II. Young-Wook Kim acknowledges partial support from a National Research Foundation of Korea (NRF) funded by Ministry of Science, ICT & Future Planning (Grant number: 2016K1A3A1A19945992).

References

[1] Ferraris M, Salvo M, Casalegno V, Ciampichetti A, Smeacetto F, Zucchetti M. Joining of machined SiC/SiC composites for thermonuclear fusion reactors. *J Nucl Mater* **375**(3): 410–415 (2008)

[2] MatsunagaT, Singh M, Asthana R, Lin H T, Kajii S, Ishikawa T. Microstructure and mechanical properties of joints in sintered SiC fiber-bonded ceramics. *Key Eng Mater* **484**: 9–14 (2011)

[3] Salvo M, Rizzo S, Casalegno V, Handrick K, Ferraris M. Shear and bending strength of SiC/SiC joined by a modified commercial adhesive. *Int J Appl Ceram Technol* **9**(4): 778–785 (2012)

[4] Seo Y K, Kim Y W, Nishimura T, Seo W S. High thermal conductivity of spark plasma sintered silicon carbide ceramics with Yttria and Scandia. *J Am Ceram Soc* **100**(4): 1290–1294 (2017)

[5] Zhao X Y, Liu Y, Wen Q F, Wang Y M. Frictional performance of silicon carbide under different lubrication

conditions. *Friction* **2**(1): 58–63 (2014)

[6] Sharma S K, Kumar B V M, Kim Y W. Tribological behavior of silicon carbide ceramics-a review. *J Korean Ceram Soc* **53**(6): 581–596 (2016)

[7] Cho S J, Um C D, Kim S S. Wear and wear transition in silicon carbide ceramics during sliding. *J Am Ceram Soc* **79**(5): 1247–1251 (1996)

[8] Kovalčíková A, Balko J, Dusza J. Influence of microstructure on tribological properties and nanohardness of silicon carbide ceramics. *Key Eng Mater* **662**: 55–58 (2015)

[9] Ciudad E, Borrero-López O, Ortiz A L, Guiberteau F. Microstructural effects on the sliding-wear resistance of pressureless liquid-phase-sintered SiC under diesel fuel. *J Eur Ceram Soc* **33**(4): 879–885 (2013)

[10] Borrero-López O, Ortiz A L, Guiberteau F, Padture N P. Effect of microstructure on sliding-wear properties of liquid-phase-sintered α-SiC. *J Am Ceram Soc* **88**(8): 2159–2163(2005)

[11] Sharma S K, Kumar B V M, Lim K Y, Kim Y W, Nath S K. Erosion behavior of SiC-WC composites. *Ceram Int* **40**(5): 6829–6839 (2014)

[12] Sharma S K, Kumar B V M, Kim Y W. Effect of WC addition on sliding wear behavior of SiC ceramics. *Ceram Int* **41**(3): 3427–3437 (2015)

[13] Gahr K H Z, Blattner R, Hwang D H, Pöhlmann K. Micro-and macro-tribological properties of SiC ceramics in sliding contact. *Wear* **250**(1-2): 299–310 (2001)

[14] Murthy V S R, Kobayashi H, Tsurekawa S, Tamari N, Watanabe T, Kato K. Influence of humidity and doping elements on the friction and wear of SiC in unlubricated sliding. *Tribol Int* **37**(5): 353–364 (2004)

[15] Takadoum J, Zsiga Z, Roques-Carmes C. Wear mechanism of silicon carbide: New observations. *Wear* **174**(1-2): 239–242 (1994)

[16] Skopp A, Woydt M. Ceramic-ceramic composite materials with improved friction and wear properties. *Tribol Int* **25**(1): 61–70 (1992)

[17] Kumar B V M, Kim Y W, Lim D S, Seo W S. Influence of small amount of sintering additives on unlubricated sliding wear properties of SiC ceramics. *Ceram Int* **37**(8): 3599–3608 (2011)

[18] Hsu S M, Shen M C. Ceramic wear maps. *Wear* **200**(1-2): 154–175 (1996)

[19] Kovalčíková A, Kurek P, Balko J, Dusza J, Šajgalík P, Mihaliková M. Effect of the counterpart material on wear characteristics of silicon carbide ceramics. *Int J Refrac Met Hard Mater* **44**: 12–18 (2014)

[20] Andersson P, Blomberg A. Instability in the tribochemical wear of silicon carbide in unlubricated sliding contacts. *Wear* **174**(1-2): 1–7 (1994)

[21] Cranmer D C. Friction and wear properties of monolithic silicon-based ceramics. *J Mater Sci* **20**(6): 2029–2037 (1985)

[22] Zhou Y, Hirao K, Yamauchi Y, Kanzaki S. Tribological properties of silicon carbide and silicon carbide–graphite composite ceramics in sliding contact. *J Am Ceram Soc* **86**: 991–1002 (2003)

[23] Wasche R, Klaffke D, Troczynski T. Tribological performance of SiC and TiB_2 against SiC and Al_2O_3 at low sliding speeds. *Wear* **256**(7-8): 695–704 (2004)

[24] Wäsche R, Klaffke D. In situ formation of tribologically effective oxide interfaces in SiC-based ceramics during dry oscillating sliding. *Tribol Lett* **5**(2-3): 173–190 (1998)

[25] Gupta S, Sharma S K, Kumar B V M, Kim Y W. Tribological characteristics of SiC ceramics sintered with a small amount of yttria. *Ceram Int* **41**(10): 14780–14789 (2015)

[26] Borrero-López O, Ortiz A L, Guiberteau F, Padture N P. Sliding-wear-resistant liquid-phase-sintered SiC processed using α-SiC starting powders. *J Am Ceram Soc* **90**(2): 541–545 (2007)

[27] Wang Y X, Wang L P, Xue Q J. Improvement in the tribological performances of Si_3N_4, SiC and WC by graphite-like carbon films under dry and water-lubricated sliding conditions. *Surf Coat Technol* **205**(8-9): 2770–2777 (2011)

[28] Anstis G R, Chantikul P, Lawn B R, Marshall D B. A critical evaluation of indentation techniques for measuring fracture toughness: I, direct crack measurements. *J Am Ceram Soc* **64**(9): 533–538 (1981)

[29] Kumar B V M, Basu B, Vizintin J, Kalin M. Tribochemistry in sliding wear of TiCN-Ni-based cermets. *J Mater Res* **23**(5): 1214–1227 (2008)

[30] Cortés A, Celedón C, Zarate R. CVD synthesis of graphene from acetylene catalyzed by a reduced CuO thin film deposited on SiO_2 substrates. *J Chil Chem Soc* **60**(2): 2911–2913 (2015)

[31] Luo J Y, Chen X X, Li W D, Deng W Y, Li W, Wu H Y, Zhu L F, Zeng Q G. Variable-temperature Raman spectroscopic study of the hydrogen sensing mechanism in Pt-WO_3 nanowire film. *Appl Phy Lett* **102**(11): 104–113 (2013)

[32] Anspoks A, Kalinko A, Timoshenko J, Kuzmin A. Local structure relaxation in nanosized tungstates. *Solid State Commun* **183**: 22–26 (2014)

[33] Zhang X, Niu Y A, Meng X D, Li Y, Zhao J P. Structural evolution and characteristics of the phase transformations between α-Fe_2O_3, Fe_3O_4 and γ-Fe_2O_3 nanoparticles under reducing and oxidizing atmospheres. *CrystEngComm* **15**(40): 8166–8172 (2013)

[34] Qian J W, Peng Z J, Wu D Z, Fu X L. $FeWO_4$/FeS core/shell

nanorods fabricated by thermal evaporation. *Mater Lett* **122**: 86–89 (2014)

[35] Kumar B V M, Basu B, Kalin M, Vizintin J. Load-dependent transition in sliding wear properties of TiCN–WC–Ni cermets. *J Am Ceram Soc* **90**(5): 1534–1540 (2007)

[36] Gahr K H Z, Bundschuh W, Zimmerlin B. Effect of grain size on friction and sliding wear of oxide ceramics. *Wear* **162-164**: 269-279 (1993)

[37] Rice R W. Micromechanics of microstructural aspects of ceramic wear. In *Proceedings of the 9th Annual Conference on Composites and Advanced Ceramic Materials: Ceramic Engineering and Science Proceedings*. Smothers W, Ed. Cocoa Beach, Florida: The American Ceramic Society, 1985: 940–958.

[38] Gahr K H Z. Sliding wear of ceramic-ceramic, ceramic-steel and steel-steel pairs in lubricated and unlubricated contact. *Wear* **133**(1): 1–22 (1989)

[39] Varenberg M. Towards a unified classification of wear. *Friction* **1**(4): 333–340 (2013)

[40] Tatarko P, Kašiarová M, Dusza J, Morgiel J, Šajgalík P, Hvizdoš P. Wear resistance of hot-pressed Si_3N_4/SiC micro/nanocomposites sintered with rare-earth oxide additives. *Wear* 269(11-12): 867–874 (2010)

[41] Miyazaki H, Hyuga H, Yoshizawa Y I, Hirao K, Ohji T. Correlation of wear behavior and indentation fracture resistance in silicon nitride ceramics hot-pressed with alumina and yttria. *J Eur Ceram Soc* **29**(8): 1535–1542 (2009)

Sandan Kumar SHARMA. He received his bachelors degree in mechanical engineering in 2010 from T.I.T. Bhopal, RGPV, India. He achieved his master degree in metallurgical and materials engineering at Indian Institute of Technology (IIT) Roorkee in 2012. He has recently obtained his Ph.D. degree from IIT Roorkee. His research interest includes processing of advance ceramics and their tribology.

B. Venkata MANOJ KUMAR. He is currently working as Associate Professor at the Department of Metallurgical and Materials Engineering, Indian Institute of Technology (IIT) Roorkee. He obtained Ph.D. from Indian Institute of Technology (IIT) Kanpur in materials and metallurgical engineering in 2007. After working one year as post-doctoral researcher at Seoul National University and two years as Research Assistant Professor at University of Seoul, he joined IIT Roorkee, India as Assistant Professor in 2011. Dr. Manoj works in understanding the microstructure-mechanical property-wear relation of important ceramics/cermets and composites prepared using advanced sintering techniques.

Young-Wook KIM. He received his M.S. and Ph.D. degrees in materials science and engineering from the Korea Advanced Institute of Science and Technology (KAIST), Korea, in 1983 and 1990, respectively. Before joining the University of Seoul in 1996, he worked as a senior research scientist at the Korea Institute of Science and Technology (1990–1996). His current position is a professor of materials science and engineering at University of Seoul. His research interests include the microstructural control of nonoxide ceramics, the mechanical, tribological, electrical and thermal properties of SiC ceramics, and the processing of SiC membranes.